1 **Title**

2 Multimodal imaging brain markers in early adolescence are linked with a physically active

3 lifestyle

4

5 **Authors**

6 Piergiorgio Salvan [a,*], Thomas Wassenaar [a], Catherine Wheatley [a],

7 Nicholas Beale [b], Michiel Cottaar [a], Daniel Papp [a], Matteo Bastiani [c,d,a], Sean Fitzgibbon [a],

8 Euguene Duff [a], Jesper Andersson [a], Anderson M. Winkler [e,f],

9 Gwenaëlle Douaud [a], Thomas E. Nichols [g,a,h], Stephen Smith [a], Helen Dawes [b], Heidi

10 Johansen-Berg [a]

11

12 **Affiliations**

13 a Wellcome Centre for Integrative Neuroimaging, FMRIB Centre, Nuffield Department of

14 Clinical Neurosciences, University of Oxford, John Radcliffe Hospital, OX3 9DU, United

15 Kingdom

16 b Centre for Movement, Occupational and Rehabilitation Sciences (MOReS), Oxford

17 Brookes University, Headington Campus, Oxford OX3 0BP

18 c Sir Peter Mansfield Imaging Centre, School of Medicine, University of Nottingham, United

19 Kingdom

20 d NIHR Biomedical Research Centre, University of Nottingham, UK

21 e Emotion and Development Branch, National Institute of Mental Health, National Institutes

22 of Health, Bethesda, Maryland

23 f Department of Psychiatry, Yale University School of Medicine, New Haven, Connecticut

1 g Oxford Big Data Institute, Li Ka Shing Centre for Health Information and Discovery,

2 Nuffield Department of Population Health, University of Oxford, Oxford, OX3 7LF

3 h Department of Statistics, University of Warwick, Coventry, CV4 7AL

4

5 * Corresponding author: Piergiorgio Salvan

6 Wellcome Centre for Integrative Neuroimaging

7 Nuffield Department of Clinical Neurosciences

8 University of Oxford

9 Oxford OX3 9DU

10 United Kingdom

11 E-mail: piergiorgio.salvan@ndcn.ox.ac.uk

1   **Abstract**

2   The World Health Organization (WHO) promotes physical exercise and a healthy lifestyle as

3   means to improve youth development. However, relationships between physical lifestyle and

4   brain development are not fully understood. Here, we asked whether a brain – physical latent

5   mode of covariation underpins the relationship between physical activity, fitness, and

6   physical health measures with multimodal neuroimaging markers. In 50 12-year old school

7   pupils (26 females), we acquired multimodal whole-brain MRI, characterizing brain

8   structure, microstructure, function, myelin content, and blood perfusion. We also acquired

9   physical variables measuring objective fitness levels, 7-days physical activity, body-mass

10   index, heart rate, and blood pressure. Using canonical correlation analysis we unravel a

11   latent mode of brain – physical covariation, independent of demographics, school, or

12   socioeconomic status. We show that MRI metrics with greater involvement in this mode also

13   showed spatially extended patterns across the brain. Specifically, global patterns of greater

14   grey matter perfusion, volume, cortical surface area, greater white matter extra-neurite

15   density, and resting state networks activity, covaried positively with measures reflecting a

16   physically active phenotype (high fit, low sedentary individuals). Showing that a physically

17   active lifestyle is linked with systems-level brain MRI metrics, these results suggest

18   widespread associations relating to several biological processes. These results support the

19   notion of close brain-body relationships and underline the importance of investigating

20   modifiable lifestyle factors not only for physical health but also for brain health early in

21   adolescence.

22

23   **Significance statement**

1   An active lifestyle is key for healthy development. In this work, we answer the following

2   question: How do brain neuroimaging markers relate with young adolescents' level of

3   physical activity, fitness, and physical health? Combining advanced whole-brain multimodal

4   MRI metrics with computational approaches, we show a robust relationship between

5   physically active lifestyles and spatially extended, multimodal brain imaging derived

6   phenotypes. Suggesting a wider effect on brain neuroimaging metrics than previously

7   thought, this work underlies the importance of studying physical lifestyle, as well as other

8   brain – body relationships in an effort to foster brain health at this crucial stage in

9   development.

1 Introduction

2 The World Health Organisation (WHO) encourages early positive lifestyle choices aimed to

3 improve both physical and mental health (World Health Organization 2010). Physical

4 activity is a powerful and rapid means to improve fitness and physical health throughout the

5 life-span (Cotman 2002; Charles H. Hillman, Erickson, and Kramer 2008) . During

6 adolescence, however, levels of physical activity decline (Guthold et al. 2020).

7 Public health guidelines recommend that school-aged children engage in 60 minutes of

8 moderate-to-vigorous physical activity daily (Piercy and Troiano 2018), yet globally only

9 around 22% of boys and 15% of girls achieve that (Guthold et al. 2020). In addition to its

10 importance to physical health, there is growing evidence that a physically active lifestyle

11 during childhood is associated with improved mental and cognitive health through adulthood

12 (Promotion and US Department of Health & Human Services Office of Disease Prevention

13 and Health Promotion 2000). While there is limited available evidence in adolescents, similar

14 patterns have been reported (Lubans et al. 2016).

15 A body of work has studied the relationship between single physical measures of activity,

16 fitness, or body-mass, and separate MRI metrics of brain structure, microstructure, or

17 function, showing focal neural correlates (for reviews see (Valkenborghs et al. 2019;

18 Donnelly et al. 2016)). However, it is unlikely that a single physical measure fully captures

19 active lifestyles, or that a single MRI metric fully quantifies the condition of the brain.

20 Rather, lifestyles are better characterized by a range of physical measures and the state of the

21 brain is better quantified by combinations of metrics.

22 Multimodal MRI can probe different aspects of brain structure and function. While each

23 metric provides an indirect probe of the underlying biology, in combination they provide

24 insights into a range of biological processes (Tardif et al. 2016). Further, these measures can

5

1   be acquired simultaneously across the whole brain. Many previous brain imaging studies of

2   physical activity and fitness have focused on the hippocampus, where changes in non-

3   invasive imaging measures of tissue volume or perfusion have been argued to relate to

4   processes of neurogenesis and angiogenesis triggered by exercise (van Praag et al. 1999;

5   Pereira et al. 2007; Chaddock et al. 2011; Thomas et al. 2012). However, in addition to such

6   focal changes, more global biological processes might also be triggered by exercise (Tardif et

7   al. 2016). It remains unknown whether whole-brain patterns of multimodal brain metrics are

8   related to cardiorespiratory fitness, physical activity, and physical health.

9   Physical activity influences physical health and contributes to physical fitness but both

10   activity and fitness may be considered part of an underlying, latent factor. In order to

11   characterize a phenotype of physical lifestyle, measuring whole-day physical activity levels

12   during a normal school week is therefore at least as important as assessing gold-standard

13   measures of cardiorespiratory fitness, such as VO2max measured on an incremental step-test

14   on a cycle ergometer.

15   In this study, in 50 12-year old pupils, we acquired multimodal whole-brain MRI metrics to

16   measure resting state networks (RSNs), grey matter (GM) volume and perfusion, cortical

17   surface (area and thickness), white-matter (WM) microstructure, and myelin content (R1 and

18   R2*), resulting in a total of 18 different metrics). These metrics are combined into

19   multimodal whole-brain phenotypes whose variation across individuals can be interrogated.

20   We also acquired a rich set of variables depicting physical lifestyle, measuring

21   cardiorespiratory fitness (VO2max and workload), objective physical activity (7-days

22   actigraphy, measuring total week time of brief bursts and long-lasting physical activity) and

23   reported (questionnaire item), and physical health (resting heart rate, blood pressure, and

24   body-mass index) (**Fig. 1**). We hypothesised that across pupils, inter-subject differences in

25   brain phenotypes covaried with differences in physical lifestyle, independent of sex,

6

1   socioeconomic status, age, pubertal level, and school. A single holistic multivariate analysis

2   allowed us to identify a latent mode of covariation between brain and physical phenotypes,

3   representing a pattern of active physical lifestyle features that significantly covaries with

4   spatially extended patterns of brain metrics.

5

6   **Materials and methods**

7

8   *Participants*

9   Year 7 pupils from a subset of 10 UK schools participating in the Fit to Study project, were

10   invited to take part in a brain imaging substudy (Wassenaar et al. 2019). After taking consent

11   and assent in accordance with the University of Oxford ethical guidelines (CUREC reference

12   number: R51313/RE001), 61 pupils were recruited to the brain imaging substudy.

13   Participants attended a testing session at the University of Oxford during which brain

14   imaging, cognitive, and behavioral data were collected.

15   Only 50 pupils (median age: 12 years; 26 females (52%)) (**Table 1**), had high-quality,

16   complete multimodal MRI data. All statistical analyses were carried out on this sample of 50

17   pupils sampled from 10 schools (**Table 2**).

18

19   *Behavioral testing*

20   *Cardiorespiratory fitness*

21   Objective measures of *cardiorespiratory fitness* were acquired through an incremental step-

22   test on a cycle ergometer (Lode Excalibur Sport, Groningen, The Netherlands). We then

23   extracted values for maximal oxygen consumption per kilogram (VO2/kg max) (ml/min/kg),

24   and work load maximum (Watts) as primary measures of interest.

25

1   *Physical activity*

2   Objective *physical activity* was assessed over five weekdays and 2 weekend days using the

3   Axivity AX3 wrist-worn accelerometer (Open Lab, Newcastle University, UK) (Ladha et al.

4   2013). We therefore chose to define a valid wear day as 12 consecutive hours from 08.00 to

5   20.00 to capture travel to and from school and after-school sports and activities. To account

6   for later weekend waking times, we accepted any consecutive ten-hour period between 08.00

7   and 20.00 on Saturdays and Sundays, and standardised total activity to 12 hours. We then

8   aimed to capture both *brief bursts* and *long-lasting* activity. We converted raw accelerometer

9   data into activity 'counts' per 60-second epoch and also per 1-second epoch to characterize

10   sustained bouts of activity and also shorter bursts of movement. Axivity's Open Movement

11   GUI software calculated whether each 60-second epoch was spent in sedentary, light,

12   moderate or vigorous activity by applying established adolescent cut-points (Phillips, Parfitt,

13   and Rowlands 2013). The software identified non-wear time as periods of at least 30

14   consecutive minutes of zero activity counts. We used a bespoke programme, designed to

15   handle large volumes of data, to apply the same cut-points to each 1-second epoch.

16   Participants who had at least 3 valid weekdays and one valid weekend day were included in

17   the analysis (Troiano et al. 2014). For both *brief bursts* and *long-lasting* physical activity,

18   participants' total minutes of sedentary, moderate and vigorous activity per day were

19   calculated.

20

21   *Physical health*

22   *Physical health* was assessed on the day of testing at rest (prior cardiorespiratory testing) by

23   measuring heart rate; systolic and diastolic blood pressure. When compared to publicly

24   available age-matched normative values (Flynn JT et al. 2018), blood pressure (5_{th} to 95_{th}

25   percentiles) was found within healthy values (normative values for 12 years old pupils:

8

1   *systolic*: 102-131 with average of 113; *diastolic*: 61-83 with average of 75; study sample,

2   *systolic*: median = 106, 5th-95th percentiles: 89-123; *diastolic*: median = 73, 5th-95th

3   percentiles: 58-85).

4   *Negative behaviors not considered in the analysis*

5   As part of the study we also obtained ethics to ask pupils information about negative

6   behaviors such as smoking, drinking alcohol, or drug use. However, none of the pupils

7   reported having used any of these substances.

8

9   *MR Imaging*

10   *MRI acquisition parameters*

11   All Magnetic Resonance Imaging (MRI)-scans were carried out during summer 2017 at the

12   Oxford Centre for Functional MRI of the Brain (FMRIB) using a 3T Siemens Magnetom

13   Prisma (Erlangen, Germany) scanner with a 32-channel head coil.

14   The MRI protocol included:

15   1. T1 weighted (T1w) three-dimensional rapid gradient echo sequence (3D MPRAGE):

16   repetition time (TR) = 1900 ms; echo time (TE) = 3.97 ms; flip angle = 8°; field-of-

17   view (FOV) = 192 mm; voxel size: $1\times 1 \times 1$ mm. Sequence duration: 5 min 31 sec.

18   2. Resting-state functional MRI (rs-fMRI): multi-band echo-planar imaging (EPI)

19   sequence; TR = 933ms; TE = 33.40 ms; FOV = 192 mm; 72 slices; voxel size: 2 x 2 x

20   2 mm; multi-band acceleration factor = 6. Sequence duration: 10 min 10 sec. For each

21   scan, 644 volumes were acquired. Participants were asked to look at a fixation cross,

22   blink normally, try not to fall asleep and not to think about anything in particular. A

23   field map was also acquired to correct for inhomogeneity distortions. Sequence

24   duration: 1 min 34 sec.

3. Diffusion-weighted MRI (DW-MRI): multi-shell, multi-band EPI sequence; b-values = 0, 1250, 2500 s/mm2, with respectively 11, 60, 60 diffusion-weighted directions; TR = 2483 ms; TE = 78.20 ms; FOV = 214 mm; voxel size: 1.75 x 1.75 x 1.75 mm; multi-band acceleration factor = 4. Sequence duration: 5 min 40 sec. In addition, 4 b = 0 s/mm2 images were acquired with reversed phase encoding, for the purpose of EPI distortion correction. Sequence duration: 32 sec.

4. Quantitative FLASH-MRI (Weiskopf et al. 2013): two 3D multi-echo FLASH datasets, one predominantly proton-density weighted (PDw, flip angle = 6 deg), and one predominantly T1w (flip angle = 21 deg); FOV = 256 mm; voxel size: $1 \times 1 \times 1$ mm; TR = 25 ms; first TE = 2.34 ms; eight equally space echoes, echo spacing = 2.3; GRAPPA acceleration factor = 2 in both phase-encoded directions, with 40 reference lines in each direction. Duration for each FLASH sequence: 5 min 11 sec. Two single-echo, low-resolution (4 mm isotropic) FLASH scans were acquired before each high-resolution scan; identical FOV; TR = 4 ms; TE = 2 ms; one was acquired receiving on the 32-channel receive head coil, the other receiving on the body coil. To correct for the effect of RF inhomogeneities, the local RF field was mapped using a 2D DAM method with a FLASH readout.

5. Pseudo-continuous arterial spin labeling (pCASL) with background pre-saturation (Okell et al. 2013): six imaging blocks, each with different post-labeling delays: 0.25, 0.5, 0.75, 1, 1.25 and 1.5 s. Arterial blood was magnetically tagged using a labeling duration of 1.4 s. Other imaging parameters were: single shot EPI; TR = 4100 ms; TE = 14 ms; FOV = 220 mm; voxel size: $3.4 \times 3.4 \times 4.5$ mm. Sequence duration: 5 min 34 sec.

MRI preprocessing

10

1   MRI data was processed primarily using FSL software (Jenkinson et al. 2012) and FreeSurfer

2   (Dale, Fischl, and Sereno 1999).

3   *Gradient distortion correction.* Gradient distortion correction (GDC) was applied within

4   image analysis pipelines using tools developed by FreeSurfer and HCP groups

5   (https://github.com/Washington-University/Pipelines), using the Siemens scanner specific

6   table of gradient nonlinearities.

7   *Structural.* Brain extraction was performed in native space after GDC unwarping using FSL

8   BET (Smith 2002). Tissue-type segmentation was estimated based on FSL FAST (Zhang,

9   Brady, and Smith 2001), providing hard segmentation as well as partial-volume images for

10   each tissue type. This tool was also used to provide a fully bias-field-corrected version of

11   brain extracted structural brain images. Subcortical structures were modelled using FSL

12   FIRST (Patenaude et al. 2011).

13   *Cortical surface reconstruction.* Subject-specific cortical surface reconstruction and cortical

14   parcellation were estimated based on the GDC, brain extracted T1 image, using the command

15   *recon-all* from FreeSurfer (Dale, Fischl, and Sereno 1999).

16   *Registration.* Rigid registrations between multimodal MRI native spaces were estimated

17   through FSL FLIRT with boundary-based cost function (Jenkinson et al. 2002; Greve and

18   Fischl 2009). Nonlinear warps to MNI152 standard-space T1 template were estimated

19   through FSL FNIRT. This set of nonlinear warps is then carried over to all MRI modalities

20   such as in the case of resting state functional MRI (rs-fMRI).

21   *EPI distortion correction.* B0 fieldmap processing was estimated through FSL Topup

22   (Andersson, Skare, and Ashburner 2003) based on AP-PA image pairs from DWI-MRI

23   protocol.

24   *Functional.* rs-fMRI data was preprocessed using a custom pipeline previously validated on

25   developmental datasets (Baxter et al. 2019). rs-fMRI data was corrected for inter- and intra-

1 volume subject head motion, EPI distortions (Andersson and Sotiropoulos 2015); highpass

2 temporal filtering and GDC unwarping was also applied. Registration to structural was

3 improved by an extra rigid registration step aided by a single-band EPI image. Structured

4 artefacts were removed by FSL ICA+FIX processing (Beckmann and Smith 2004; Salimi-

5 Khorshidi et al. 2014; Griffanti et al. 2014). The FSL FIX classifier was specifically trained

6 for this data and provided the following scores in leave-one subject-out accuracy: true

7 positive ratio (TPR) = 98.8%; true negative ratio (TNR) = 95.3%; weighted ratio (

8 (3*TPR+TNR)/4) = 97.9%. FSL MELODIC was then used to estimate 50 group-average

9 independent components (ICs). We then calculated median absolute (ridge) partial correlation

10 (with a regularization value of 0.1) and amplitude for each of the 25 ICs identified as RSNs.

11 *Diffusion.* DWI-MRI data was first corrected for eddy currents, EPI distortions, inter- and

12 intra-volume subject head motion, with outlier-slice replacement, using FSL Eddy

13 (Andersson and Sotiropoulos 2015). GDP unwarping was then applied (Miller et al. 2016).

14 Diffusion Tensor Imaging (DTI) fitting was carried out with FSL DTIFIT using a kurtosis

15 model (Behrens et al. 2007). Neurite Orientation Dispersion and Density Imaging (NODDI)

16 modelling was estimated using FSL cuDIMOT

17 (https://users.fmrib.ox.ac.uk/~moisesf/cudimot/DesignModel.html) based on the Bingham-

18 NODDI model (Tariq et al. 2016). In order to resolve crossing-fibres configurations, multi-

19 shell voxel-wise diffusion was modelled using FSL BedpostX (Jbabdi et al. 2012).

20 Probabilistic tractography was then carried out with FSL ProbtrackX (Behrens et al. 2007)

21 and 29 major WM bundles were reconstructed as implemented in FSL AutoPtx (de Groot et

22 al. 2013) [31].

23 *Myelin and iron maps*. Quantitative MRI data was processed to produce the quantitative

24 maps of myelination (1/T1) and iron level (1/T2*), using the Voxel-Based Quantification

25 (VBQ) toolbox (Callaghan et al. 2014) in Statistical Parametric Mapping (SPM)

12

1   (http://www.fil.ion.ucl.ac.uk/spm/). Although R1 (1/T1, longitudinal relaxation rate) and R2*

2   (1/T2*, effective transverse relaxation rate) are not *direct* quantitative maps of myelination or

3   iron (as other biological factors can also affect them), these quantitative maps have high

4   degree of sensitivity to myelination and iron (Weiskopf et al. 2013; Lutti et al. 2014;

5   Callaghan et al. 2014) .

6   *Perfusion*. Perfusion images were processed using FSL BASIL (Chappell et al. 2009). Images

7   were first corrected with fieldmap and GDC unwarping; then, in order to obtain maps of

8   cerebral blood flow and arrival time in absolute units, a calibration step was implemented

9   based on cerebrospinal fluid values.

10

11 *Image derived phenotypes (IDPs)*

12 Each MRI parameter was summarized in a series of IDPs: anatomy-specific average values

13 that span three sets of regions of interest. For cortical and subcortical regions, we used the

14 Desikan-Killiany Atlas (84 parcels, cortical and subcortical) from the individual FreeSurfer

15 parcellation (Fischl et al. 2002). This parcellation was then warped into each (relevant)

16 modality in order not to interpolate MRI-map values. For the white matter, we used the 29

17 white-matter bundles from the AutoPtx reconstruction; first averaged at group-level;

18 optimally thresholded; and then warped back to native spaces. For functional activity, 25

19 group-level RNSs were identified.

20 A total of 859 IDPs were then fed into statistical analysis.

21

22 *Cognitive testing and reported mental health and general health measures*

23 All measures acquired during the testing are reported in detail in (Wassenaar et al. 2019).

24

25 *Cognitive skills*

1   Here we considered a summary measure for 3 tasks of interest: the relational memory task

2   (correct valid answers (%)) (Chaddock et al. 2010); task switching (switch cost (ms)) (C. H.

3   Hillman et al. 2014) ; and object-location task (identification errors 8s-delay) (Pertzov et al.

4   2012), (**Table 3**).

5

6   *Mental health*

7   Mental health was assessed with the Strengths and Difficulties Questionnaire (SDQ)

8   (Goodman 1997).

9

10   *Questionnaire on general health*

11   From the Health behavior in school-age children (HSBC) questionnaire *(World Health*

12   *Organization. Regional Office for Europe 2016)* we used the positive health items (self-rated

13   health, life satisfaction, multiple health complaints) in order to measure reported general

14   health.

15

16   *Experimental design and statistical analyses*

17   This is a cross-sectional study with a sample size of N = 50 subjects. Due to the limited

18   sample size compared to the number of variables of interest, we strove to reduce input data

19   and nuisance variables dimensions as much as possible. All statistical analyses were carried

20   out in MATLAB 2018.

21

22   *Confounds*

23   Prior to all statistical analyses, a series of relevant confounds was chosen: age; sex; pubertal

24   developmental level (assessed through the *Pubertal Development Rating Scale* (Petersen et

25   al. 1988), a self-report measure of physical development for youths under the age of 16);

14

1   socioeconomic status (assessed through the UK Index of Multiple Deprivation); and head

2   size/scaling factor (computed through FSL SIENAX).

3   On these nuisance variables we perform a dimensionality reduction through means of

4   principal component analysis (PCA) ($Nz = 2$) accounting for 60% of total variance. These

5   confounds were then regressed out of all IDPs and behavioral variables and the residuals

6   normalised.

7

8   *Dimensionality reduction of IDPs and physical variables*

9   In order to avoid an overdetermined, rank deficient CCA solution, and to limit the chances of

10   overfitting, a dimensionality reduction set was performed to both IDPs and physical

11   variables. Using the same approach previously applied in (Smith et al. 2015), IDPs were

12   reduced into 10 PCAs ($Nx = 10$; variance explained = 53%), whilst physical variables were

13   reduced into 5 PCAs ($Ny = 5$; variance explained = 79%).

14

15   *Canonical correlation analysis*

16   We sought to characterize a mode of brain – physical covariation across pupils: a data-driven

17   latent factor linking a linear combination of neuroimaging metrics (**Table 4**) with a linear

18   combination of physical measures (**Table 5**). To this end we used canonical correlation

19   analysis (CCA), an approach that has successfully been applied in recent studies and that,

20   compared to pairwise association testing, has shown greater sensitivity for complex

21   biological processes and greater explained variance (Miller et al. 2016; Smith et al. 2015).

22   CCA is a symmetric, cross-decomposition method that characterizes covariation modes

23   between a pair of two-dimensional datasets. This is achieved by finding two sets of free

24   parameters (or *canonical coefficients*, i.e. one set of coefficient vectors per set of brain

25   metrics and one set of coefficient vectors per set of physical metrics) that maximize the

1   correlation of the projections of the two datasets into the identified latent space (or *canonical*

2   *variates* or subject *scores*). In other words, the variation in mode strength between subjects is

3   maximally correlated. Here, this was computed using MATLAB 'canoncorr' function.

4

5   *Unbiased statistical inference through block-aware permutation testing*

6   Deconfounding, as required to ensure that the CCA is not driven by nuisance factors, induces

7   a dependency among the rows of the data submitted to CCA. While this dependency is weak

8   and diminishes with increasing sample size, it represents a violation of the exchangeability

9   assumption required by permutation, that can inflate permutation significance. To account for

10 this deconfounding-induced dependency that violates exchangeability, we use a method that,

11 without changing the canonical correlations, reduces the data from N observations to N-Nz

12 observations that are exchangeable, and thus, can be subjected to a permutation test (Winkler

13 et al. 2020; Theil 1965). We randomly chose 1,000 sets of Nz rows for removal, conducting

14 1,000 permutations for each set.

15 Permutations were performed among subjects within school, respecting dependencies given

16 by the hierarchical structure of the data (Winkler et al. 2015). For each of the 1,000

17 repetitions, a *p*-value was computed based on this null distribution for the first CCA mode.

18 Across repetitions, a distribution of statistical significance values was built and the final

19 statistical significance level was computed as its average value. The results of this analysis

20 are shown in **Fig. 2b**.

21

22 *Unbiased estimation of effect size through leave-one school-out cross-validation*

23 In order to derive an unbiased estimate of the CCA correlation strength that took into account

24 the hierarchical structure in the data, we implemented a leave-one school-out cross-validation

25 (CV) approach. In all but one school, we performed all the above steps (except permutation

16

1   testing), learning all the coefficients of the linear transformations. On the left-out school, we

2   then applied those transformations and predicted left-out pupils' scores in the CCA mode. We

3   repeated this procedure for all folds (here schools). CV performance was then quantified as

4   the Pearson's rho correlation coefficient and mean squared error (MSE) calculated between

5   predicted brain and physical canonical covariates (or predicted canonical variates or CCA

6   subject *scores*). The results of this analysis are shown in **Fig. 2a**.

7

8   *Characterization of brain and physical phenotypes*

9   We then aimed to characterize the CCA phenotypes: the set of brain measures and the set of

10   physical measures symmetrically linked by the CCA covariance mode. To do this (formally,

11   to characterize the CCA crossed *loadings*), we follow the procedure described in (Smith et al.

12   2015). On the whole sample, CCA Brain loadings were calculated as the pairwise Pearson's

13   *partial* correlation between CCA Physical variate (or subject *scores*) and the original datasets

14   of brain IDPs, while controlling for the full set of nuisance variables (CCA Brain loadings =

15   partialcorrelation(brain IDPs, CCA Physical variate, nuisance variables). The results of this

16   process are shown in **Fig. 4, 5, 6**. CCA Physical loadings were calculated with the following

17   the same process (CCA Physical loadings = partialcorrelation(physical variables, CCA Brain

18   variate, nuisance variables). The results of this process (only for structural IDPs) are shown

19   in **Fig. 3**. CCA loadings are therefore bounded between 1 and -1.

20   For functional measures, each IDP is represented by a whole-brain RSN. To aid

21   interpretation, for each RSN, its CCA Brain loading was multiplied by the group RSN map.

22   The results of this process are shown in **Fig. 5a, b**. Then, in order to derive a summary

23   representation, we concatenated all RSNs maps in a 4D file and computed normalised mean

24   across RSNs, separately for both functional connectivity and amplitude. The results of this

25   process are shown in **Fig. 5c, d**.

1   We then aimed to characterize the average involvement for each type of MRI value. Across

2   IDPs of a MRI metric, we computed the average across CCA Brain loadings. This provided a

3   ranked list of MRI parameters representing the average relationship of each MRI metric with

4   pupils' physical scores. The results of this process are shown in **Fig. 7**.

5

6   *Joint-inferences with univariate measures of cognitive skills, mental health, and general*

7   *health*

8   The relationships between the identified CCA mode and the multiple variables measuring the

9   domains of cognitive skills, mental health, and general health, were carried out (separately

10   for each domain) with a general linear model with non-parametric combination (NPC)

11   implemented in FSL PALM (Winkler et al. 2016). NPC works by combining test statistics or

12   p-values of separate (even if not independent) analyses into a single, joint statistic, the

13   significance of which is assessed through synchronized permutations for each of the separate

14   tests. Here we asked whether the CCA mode was associated with any sub-measure within a

15   domain, and the NPC was tested via Tippett statistic with 1,000 block-aware permutations,

16   while adjusting for nuisance variables in reduced space.

17

18   **Results**

19

20   *Brain – physical mode of covariation across pupils*

21   Using CCA, we tested the hypothesis that across pupils, inter-subject differences in

22   multimodal whole-brain IDPs covaried significantly with differences in physical lifestyle

23   variables, independent of nuisance variables. We found one significant mode of brain –

24   physical covariation across pupils, linking differences in brain IDPs with individual

1   differences in physical lifestyle (**Fig. 2a**; CCA: rho = 0.34, MSE = 1.38, using leave-one

2   school-out CV; **Fig. 2b**; p-value = 0.0130, significance assessed on 1,000 repetitions, each

3   with 1,000 block-aware permutations; results remained the same if adjusted for the full set of

4   nuisance variables). This mode represents a pattern of brain IDPs that covaries with a pattern

5   of physical variables. We next interrogated this physical phenotype and brain phenotype

6   separately, to determine the patterns that underlie this mode.

7

8   *Physical phenotype of covariation*

9   For each physical variable we calculated the loadings of the physical phenotype relating to

10   the CCA mode (or 'CCA Physical loadings') representing the relationship between each

11   physical variable and the CCA brain variate (or *subjects' brain scores*) (**Fig. 3**). We found

12   that pupils who scored higher in the brain – physical mode of covariation were those with

13   higher cardiovascular fitness; those with lower body-mass index; those who spent more time

14   doing long-lasting (both moderate and vigorous) physical activity during a normal school

15   week and spent less time being sedentary.

16

17   *Brain phenotypes of covariation*

18   In order to interpret brain phenotypes of physical covariation, we calculated the canonical

19   loadings for each IDP of brain structure, microstructure, and function. These loadings (or

20   'CCA Brain loadings') represent the relationship between each brain IDP and the CCA

21   Physical variate (or *subjects' physical scores*) (to explore the spatial patterns of *all* structural

22   and functional IDPs, see respectively **Fig. 4** and **Fig. 5a, b**; for violin plot of CCA Brain

23   loadings for all IDPs, see **Fig. 6**).

19

1 We observed that some MRI metrics presented a global and homogeneous involvement in the

2 mode of covariation across ROIs. In order to quantify this tendency, for each MRI metric, we

3 computed the *average* CCA Brain loadings across all ROIs (**Fig. 7**). We found that the

4 strongest CCA Brain loadings were found for GM perfusion (and arrival time) as well as

5 cortical surface area, GM volume and a number of WM diffusion metrics. MRI metrics with

6 the greatest average CCA Brain loadings tended to be characterized by spatially extended and

7 homogeneous involvement across the whole-brain. Together, these results show that pupils

8 with greater physical scores were those who also showed global patterns of higher blood

9 perfusion (and lower arrival time, i.e., faster perfusion) in the GM, greater GM volume,

10 greater cortical surface area, greater neurite dispersion anisotropy across WM tracts, as well

11 as greater extra-neurite fraction (equivalent to lower *intra*-neurite fraction), and lower neurite

12 orientation dispersion.

13 We also observed that although the *average* CCA Brain loadings for RSNs functional

14 connectivity and BOLD amplitude was close to zero, there was great variance across RSNs

15 (**Fig. 5**). Because RSNs are not binary masks but are instead characterized by spatial

16 distributions, in order to summarise their pattern of involvement in the mode of covariation,

17 for each voxel we computed the normalised mean CCA Brain loadings across RSNs (**Fig. 5c,**

18 **d**). The resulting maps for functional connectivity (**Fig. 5c**) and amplitude (**Fig. 5d**) showed

19 both similarities and differences in their patterns of involvement in the mode of covariation.

20 In Fig. 5.c, RSN functional connectivity shows greater positive involvement bilaterally in the

21 parietal cortices, supplementary motor cortex, putamen, and right primary motor cortex;

22 while it shows greater negative involvement broadly in the occipital cortices. The peak of

23 positive involvement was localised in the right parietal cortex, while the negative in the

24 occipital cortex. In Fig. 5d, RSN BOLD amplitude shows greater positive involvement in the

25 anterior cingulate gyrus (dACC), superior frontal gyrus, parietal cortices, right inferior frontal

20

1 gyrus; while it shows greater negative involvement broadly in the occipital cortices, and left

2 primary somatosensory cortex. The peak of positive involvement was localised in the dACC,

3 while the negative in the occipital cortex. These maps show a common pattern of greater

4 positive involvement bilaterally in the parietal cortices, and a common pattern of negative

5 involvement in the occipital cortices.

6

7 *Relationship with measures of cognition, mental health, and general health*

8 We then tested the hypothesis that the identified CCA mode of brain – physical covariation

9 (averaging between brain and physical CCA subjects scores), was significantly associated

10 with measures of 1) cognitive skills, 2) mental health, and 3) general reported health. Testing

11 a NPC joint-inference for each domain, we found no statistically significant association (NPC

12 Tippett p-value respectively for cognitive skills: p-value = 0.3280; mental health: p-value =

13 0.7940; general health: p-value = 0.1280).

14 Of interest for future studies, we report that one of the three HBSC questionnaire items in

15 general reported health (*self-rated health*) was positively associated with the mode of brain –

16 physical covariation if not corrected for multiple comparisons across the three items tested

17 (Adjusted R2 = 0.16, p-value = 0.0430).

18 Importantly, when not using block-aware permutations and thus not taking into account the

19 hierarchical structure represented by schools, the association between the mode of brain –

20 physical covariation and the domain of general health was found to be significant. This

21 highlights the importance of considering schools' effect (or any other hierarchical structure)

22 when testing associations across a population. It also emphasizes how robust the results from

23 the brain – physical covariation are to nuisance of no interest and to hierarchical structure in

24 the data.

1

2 **Discussion**

3 In this work we show that, in 12-year-old pupils, physical activity, fitness, and physical

4 health are linked with global patterns of brain structure, microstructure, and function. In this

5 relationship, whole-brain, homogeneous patterns of multimodal brain phenotypes are linked

6 with a specific, latent pattern of physical measures that capture a physically active lifestyle

7 (high fit, high active, low sedentary individuals). This finding hints at the involvement of

8 multiple underlying biological processes and suggests that physical health and aerobic

9 exercise might have a wider effect on brain processes than previously thought.

10 We applied a holistic approach to provide novel insight into the importance of different

11 aspects of a physically active lifestyle in relation to brain structure and function. While high

12 cardiovascular fitness and physical activity are positively linked with the identified brain

13 phenotypes, sedentary activity and body-mass index are negatively related. Furthermore, we

14 showed that long-lasting physical activity, either moderate or vigorous, is more important to

15 this relationship than brief bursts of activity, suggesting that regular moderate-to-vigorous

16 physical activity might be a better driver to promote brain changes. Taken together, these

17 findings situate pupils along a latent axis according to their physical phenotype: pupils with

18 high cardiorespiratory fitness and performance and with high weekly levels of physical

19 activity, g, contrast with pupils spending most time in sedentary or low-energy behaviors.

20 The novelty of this work is the finding of multimodal global brain phenotypes linked with a

21 physically active lifestyle. Although prior work has studied the relationship between single

22 measures of brain structure or function and, separately, physical activity or fitness

23 (Valkenborghs et al. 2019), our approach allowed us to identify latent patterns of multimodal

24 brain IDPs characterized by the involvement of multiple brain regions in the covariation with

1   physical scores. Specifically, greater physical scores were linked with spatially extended

2   patterns of greater blood perfusion and faster arrival time in the GM, greater GM volume and

3   larger cortical surface area, and in the WM with lower intra-neurite density and kurtosis. This

4   result shows that high fitness and physical activity are associated with more *global* patterns

5   of brain structure than previously thought. Further work is needed to better understand

6   multimodal, spatially extended phenotypes of brain structure (Groves et al. 2012; Douaud et

7   al. 2014). Indeed it remains unknown how spatially extended brain patterns relate to

8   individual differences in cognition, their level of heritability, as well as to what extent they

9   are susceptible to plasticity. Although it is not possible to infer the presence of a specific

10   biological process or cellular component solely on the basis of MRI measures (Zatorre,

11   Fields, and Johansen-Berg 2012), these results suggest that high fitness and regular physical

12   activity might have a more *widespread* impact on brain structure than previously thought.

13   Previous literature has explicitly focused on studying the effects of aerobic exercise on the

14   hippocampus (Cotman 2002; Falkai and Schmitt 2009; Chaddock-Heyman et al. 2016;

15   Thomas et al. 2016). Cardiorespiratory fitness is indeed known to promote hippocampal

16   neurogenesis and angiogenesis that, in turn, determines macro-scale changes that are also

17   visible via non-invasive neuroimaging (van Praag et al. 1999). Here, we extend the current

18   knowledge beyond a uniquely hippocampal pattern, highlighting the global nature of greater

19   volume and faster perfusion across the whole brain GM. In other words, variation in

20   hippocampal structure alone does not underlie the brain – physical relationship characterized

21   here. Rather we observed homogeneous loadings across GM areas. The strongest

22   contributions to our brain phenotype came from perfusion measures. These robust

23   associations found with perfusion metrics are in line with a body of literature showing

24   positive effects of physically active lifestyle on vascular health (Vaynman, Ying, and Gomez-

25   Pinilla 2004; Promotion and US Department of Health & Human Services Office of Disease

1   Prevention and Health Promotion 2000), as well as animal studies linking physical exercise

2   to angiogenesis (Kleim et al. 1996; Rhyu et al. 2010).

3   Further key insights derive from spatially extended patterns of WM covariation. Although the

4   myelin sensitive metrics (Quantitative-MRI R1 and R2*) in the current study made little

5   contribution to the mode of variation, higher scores on the physical phenotype were

6   associated with lower intra-neurite density and kurtosis, and to a lesser extent with lower

7   neurite orientation dispersion and with greater dispersion anisotropy. It is relevant that the

8   DW-MRI protocol employed in this study would be sensitive to diffusion properties within

9   large glial cells, such as astrocytes and oligodendrocytes. Our gradient strength provides

10   sensitivity to length-scales of roughly 4-6 μm, with the body-size of astrocyte and

11   oligodendrocytes being respectively in the order 20 μm (Oberheim et al. 2009) and of 14 μm

12   (Bakiri et al. 2011), much larger than the average myelinated axon diameter (<1 μm)

13   (Liewald et al. 2014). Indeed astrocytes and oligodendrocytes are the most abundant cells in

14   WM (based on cell counts), accounting for more than half the volume of a MRI voxel

15   (Walhovd, Johansen-Berg, and Káradóttir 2014). It is thus possible that an increase in size or

16   number of macro-glia cells would have a significant effect on the DW-MRI signal, thus

17   contributing to the positive association here observed between physical lifestyle scores and

18   WM *extra*-neurite fraction (by construction 1 minus intra-neurite density (NODDI f-intra),

19   and specifically, the hindered space outside the neurites prescribed through anisotropic

20   diffusion). Crucially, there exists key histological evidence from animal studies in support of

21   an increase in astrocyte proliferation and in glial fibrillary acidic protein (GFAP) levels (Li et

22   al. 2005; Uda et al. 2006) and in oligodendrocytes number (Luo et al. 2019) in several areas

23   of the rat brain. Together with this previous literature, the findings here reported may suggest

24   a positive relationship between physically active lifestyle and macro-glia cell density across

25   multiple WM tracts, perhaps reflecting a role in providing enhanced metabolic support for

1   neurons. This hypothesis should be tested using imaging alongside more direct measures

2   from ex vivo studies, or using alternative techniques with greater specificity, such as

3   detecting MRS-visible metabolites with greater sensitivity to astrocytes (Brand, Richter-

4   Landsberg, and Leibfritz 1993).

5   We also report two patterns of RSNs involvement in the mode of brain – physical

6   covariation. We found that a physically active lifestyle was linked with greater connectivity

7   in the parietal cortices and with lower connectivity in the occipital cortices, showing

8   respectively increased and decreased BOLD coupling with all RSNs in more active

9   participants. The same phenotype of a physically active lifestyle was also positively related

10   with greater amplitude in local BOLD fluctuations in the dACC and in the parietal cortices,

11   and with lower amplitude in the occipital cortices. Studying both RSNs amplitude (BOLD

12   variance) and functional connectivity (BOLD covariance) can be important in order to

13   understand possible sources of change and the related neural processes (Duff et al. 2018;

14   Garrett et al. 2010). While greater activity both in functional connectivity and in BOLD

15   amplitude may suggest greater co-activation between the parietal cortices and multiple RSNs

16   across the whole-brain, greater BOLD amplitude with no increase in functional connectivity -

17   as observed in the dACC - may suggest greater local activity that results in a decoupling of

18   the dACC from the rest of brain activity. Greater dACC activity during a cognitive control

19   task was previously associated with higher fitness levels in preadolescent children, with

20   greater dACC activity in the high fit group positively related to accuracy in task performance

21   (Voss et al. 2011). In this study however, we found no significant association between pupil's

22   scores in the mode of brain – physical covariation and differences in cognitive skills or

23   mental health, thus not allowing us to infer on the cognitive or mental health relevance of this

24   brain pattern.

1   Overall, our findings lend support to the growing body of evidence demonstrating a close

2   relationship between the body and the brain. Although the relatively small sample size given

3   the number of variables of interest and the possible cluster effect of schools may represent a

4   limitation of this study, here we employed thorough statistical procedures (i.e. block-aware

5   permutation testing and leave-one cluster-out cross-validation) to explicitly deal with this

6   factor, thus producing robust and unbiased statistics. Also, the results here reported are

7   correlational and therefore caution is required in interpreting directionality. Nevertheless our

8   findings suggest that a complex physical phenotype that is influenced by physiology, and

9   lifestyle choices, might have widespread effects on biological processes influencing brain

10   phenotypes. Future studies may test whether improving physical health and fitness through

11   means of activity interventions, promotes diffuse neuroplasticity.

12   In conclusion, this work provides novel insight into the comprehensive relationship between

13   physically active lifestyle and brain structure and physiology in early adolescence. These

14   findings have broad implications for future research, suggesting novel avenues to study the

15   effect of modifiable lifestyle factors as part of wider brain-body relationships. Understanding

16   how physical pathways may foster healthy human brain development can help us to develop

17   better intervention studies aimed at informing public health and education policies.

18

19   **Author contributions**

20   P.S., T.W., and H.J.B. designed the experiment; P.S., T.W., C.W. and N.B. collected and

21   processed the data; M.C., D.P., M.B, S.F. and E.D. contributed to data processing; P.S.

22   analysed the data; T.N., S.S., A.M.W., and G.D. contributed to data analysis; and P.S. and

23   H.J.B. wrote the manuscript. All authors contributed with the interpretation of the findings

24   and in writing the manuscript.

25

1 Competing interests

2 The authors declare no competing financial interests.

3

17

18 References

19 Andersson, Jesper L. R., Stefan Skare, and John Ashburner. 2003. "How to Correct

20   Susceptibility Distortions in Spin-Echo Echo-Planar Images: Application to Diffusion

21   Tensor Imaging." *NeuroImage*. https://doi.org/10.1016/s1053-8119(03)00336-7.

22 Andersson, Jesper L. R., and Stamatios N. Sotiropoulos. 2015. "Non-Parametric

23   Representation and Prediction of Single- and Multi-Shell Diffusion-Weighted MRI Data

24   Using Gaussian Processes." *NeuroImage*.

25   https://doi.org/10.1016/j.neuroimage.2015.07.067.

1   Bakiri, Yamina, Ragnhildur Káradóttir, Lee Cossell, and David Attwell. 2011.

2   "Morphological and Electrical Properties of Oligodendrocytes in the White Matter of the

3   Corpus Callosum and Cerebellum." *The Journal of Physiology* 589 (Pt 3): 559–73.

4   Baxter, Luke, Sean Fitzgibbon, Fiona Moultrie, Sezgi Goksan, Mark Jenkinson, Stephen

5   Smith, Jesper Andersson, Eugene Duff, and Rebeccah Slater. 2019. "Optimising

6   Neonatal fMRI Data Analysis: Design and Validation of an Extended dHCP

7   Preprocessing Pipeline to Characterize Noxious-Evoked Brain Activity in Infants."

8   *NeuroImage* 186 (February): 286–300.

9   Beckmann, Christian F., and Stephen M. Smith. 2004. "Probabilistic Independent Component

10   Analysis for Functional Magnetic Resonance Imaging." *IEEE Transactions on Medical*

11   *Imaging* 23 (2): 137–52.

12   Behrens, T. E. J., H. Johansen-Berg, S. Jbabdi, M. F. S. Rushworth, and M. W. Woolrich.

13   2007. "Probabilistic Diffusion Tractography with Multiple Fibre Orientations: What Can

14   We Gain?" *NeuroImage*. https://doi.org/10.1016/j.neuroimage.2006.09.018.

15   Brand, A., C. Richter-Landsberg, and D. Leibfritz. 1993. "Multinuclear NMR Studies on the

16   Energy Metabolism of Glial and Neuronal Cells." *Developmental Neuroscience* 15 (3-

17   5): 289–98.

18   Callaghan, Martina F., Patrick Freund, Bogdan Draganski, Elaine Anderson, Marinella

19   Cappelletti, Rumana Chowdhury, Joern Diedrichsen, et al. 2014. "Widespread Age-

20   Related Differences in the Human Brain Microstructure Revealed by Quantitative

21   Magnetic Resonance Imaging." *Neurobiology of Aging*.

22   https://doi.org/10.1016/j.neurobiolaging.2014.02.008.

23   Chaddock-Heyman, Laura, Kirk I. Erickson, Michael A. Chappell, Curtis L. Johnson, Caitlin

24   Kienzler, Anya Knecht, Eric S. Drollette, et al. 2016. "Aerobic Fitness Is Associated

25   with Greater Hippocampal Cerebral Blood Flow in Children." *Developmental Cognitive*

Neuroscience 20 (August): 52–58.

Chaddock, Laura, Kirk I. Erickson, Ruchika Shaurya Prakash, Jennifer S. Kim, Michelle W. Voss, Matt VanPatter, Matthew B. Pontifex, et al. 2010. "A Neuroimaging Investigation of the Association between Aerobic Fitness, Hippocampal Volume, and Memory Performance in Preadolescent Children." *Brain Research*. https://doi.org/10.1016/j.brainres.2010.08.049.

Chaddock, Laura, Matthew B. Pontifex, Charles H. Hillman, and Arthur F. Kramer. 2011. "A Review of the Relation of Aerobic Fitness and Physical Activity to Brain Structure and Function in Children." *Journal of the International Neuropsychological Society*. https://doi.org/10.1017/s1355617711000567.

Chappell, M. A., A. R. Groves, B. Whitcher, and M. W. Woolrich. 2009. "Variational Bayesian Inference for a Nonlinear Forward Model." *IEEE Transactions on Signal Processing*. https://doi.org/10.1109/tsp.2008.2005752.

Cotman, C. 2002. "Exercise: A Behavioral Intervention to Enhance Brain Health and Plasticity." *Trends in Neurosciences*. https://doi.org/10.1016/s0166-2236(02)02143-4.

Dale, A. M., B. Fischl, and M. I. Sereno. 1999. "Cortical Surface-Based Analysis. I. Segmentation and Surface Reconstruction." *NeuroImage* 9 (2): 179–94.

Donnelly, Joseph E., Charles H. Hillman, Darla Castelli, Jennifer L. Etnier, Sarah Lee, Phillip Tomporowski, Kate Lambourne, Amanda N. Szabo-Reed, and This summary was written for the American College of Sports Medicine by. 2016. "Physical Activity, Fitness, Cognitive Function, and Academic Achievement in Children: A Systematic Review." *Medicine and Science in Sports and Exercise* 48 (6): 1223–24.

Douaud, Gwenaëlle, Adrian R. Groves, Christian K. Tamnes, Lars Tjelta Westlye, Eugene P. Duff, Andreas Engvig, Kristine B. Walhovd, et al. 2014. "A Common Brain Network Links Development, Aging, and Vulnerability to Disease." *Proceedings of the National*

29

1   *Academy of Sciences of the United States of America* 111 (49): 17648–53.

2   Duff, Eugene P., Tamar Makin, Michiel Cottaar, Stephen M. Smith, and Mark W. Woolrich.

3   2018. "Disambiguating Brain Functional Connectivity." *NeuroImage* 173 (June): 540–

4   50.

5   Falkai, Peter, and Andrea Schmitt. 2009. "Faculty Opinions Recommendation of An in Vivo

6   Correlate of Exercise-Induced Neurogenesis in the Adult Dentate Gyrus." *Faculty*

7   *Opinions – Post-Publication Peer Review of the Biomedical Literature*.

8   https://doi.org/10.3410/f.1071124.597943.

9   Fischl, Bruce, David H. Salat, Evelina Busa, Marilyn Albert, Megan Dieterich, Christian

10   Haselgrove, Andre van der Kouwe, et al. 2002. "Whole Brain Segmentation: Automated

11   Labeling of Neuroanatomical Structures in the Human Brain." *Neuron* 33 (3): 341–55.

12   Flynn JT et al. 2018. "Clinical Practice Guideline for Screening and Management of High

13   Blood Pressure in Children and Adolescents." *Pediatrics* 142 (3).

14   https://doi.org/10.1542/peds.2018-1739.

15   Garrett, Douglas D., Natasa Kovacevic, Anthony R. McIntosh, and Cheryl L. Grady. 2010.

16   "Blood Oxygen Level-Dependent Signal Variability Is More than Just Noise." *The*

17   *Journal of Neuroscience: The Official Journal of the Society for Neuroscience* 30 (14):

18   4914–21.

19   Goodman, Robert. 1997. "The Strengths and Difficulties Questionnaire: A Research Note."

20   *Journal of Child Psychology and Psychiatry*. https://doi.org/10.1111/j.1469-

21   7610.1997.tb01545.x.

22   Greve, Douglas N., and Bruce Fischl. 2009. "Accurate and Robust Brain Image Alignment

23   Using Boundary-Based Registration." *NeuroImage* 48 (1): 63–72.

24   Griffanti, Ludovica, Gholamreza Salimi-Khorshidi, Christian F. Beckmann, Edward J.

25   Auerbach, Gwenaëlle Douaud, Claire E. Sexton, Enikő Zsoldos, et al. 2014. "ICA-

Based Artefact Removal and Accelerated fMRI Acquisition for Improved Resting State Network Imaging." *NeuroImage* 95 (July): 232–47.

Groot, Marius de, Meike W. Vernooij, Stefan Klein, M. Arfan Ikram, Frans M. Vos, Stephen M. Smith, Wiro J. Niessen, and Jesper L. R. Andersson. 2013. "Improving Alignment in Tract-Based Spatial Statistics: Evaluation and Optimization of Image Registration." *NeuroImage* 76 (August): 400–411.

Groves, Adrian R., Stephen M. Smith, Anders M. Fjell, Christian K. Tamnes, Kristine B. Walhovd, Gwenaëlle Douaud, Mark W. Woolrich, and Lars T. Westlye. 2012. "Benefits of Multi-Modal Fusion Analysis on a Large-Scale Dataset: Life-Span Patterns of Inter-Subject Variability in Cortical Morphometry and White Matter Microstructure." *NeuroImage* 63 (1): 365–80.

Guthold, Regina, Gretchen A. Stevens, Leanne M. Riley, and Fiona C. Bull. 2020. "Global Trends in Insufficient Physical Activity among Adolescents: A Pooled Analysis of 298 Population-Based Surveys with 1·6 Million Participants." *The Lancet Child & Adolescent Health*. https://doi.org/10.1016/s2352-4642(19)30323-2.

Hillman, Charles H., Kirk I. Erickson, and Arthur F. Kramer. 2008. "Be Smart, Exercise Your Heart: Exercise Effects on Brain and Cognition." *Nature Reviews. Neuroscience* 9 (1): 58–65.

Hillman, C. H., M. B. Pontifex, D. M. Castelli, N. A. Khan, L. B. Raine, M. R. Scudder, E. S. Drollette, R. D. Moore, C. -T. Wu, and K. Kamijo. 2014. "Effects of the FITKids Randomized Controlled Trial on Executive Control and Brain Function." *PEDIATRICS*. https://doi.org/10.1542/peds.2013-3219.

Jbabdi, Saad, Stamatios N. Sotiropoulos, Alexander M. Savio, Manuel Graña, and Timothy E. J. Behrens. 2012. "Model-Based Analysis of Multishell Diffusion MR Data for Tractography: How to Get over Fitting Problems." *Magnetic Resonance in Medicine*.

1   https://doi.org/10.1002/mrm.24204.

2   Jenkinson, Mark, Peter Bannister, Michael Brady, and Stephen Smith. 2002. "Improved

3   Optimization for the Robust and Accurate Linear Registration and Motion Correction of

4   Brain Images." *NeuroImage* 17 (2): 825–41.

5   Jenkinson, Mark, Christian F. Beckmann, Timothy E. J. Behrens, Mark W. Woolrich, and

6   Stephen M. Smith. 2012. "FSL." *NeuroImage*.

7   https://doi.org/10.1016/j.neuroimage.2011.09.015.

8   Kleim, J. A., E. Lussnig, E. R. Schwarz, T. A. Comery, and W. T. Greenough. 1996.

9   "Synaptogenesis and Fos Expression in the Motor Cortex of the Adult Rat after Motor

10   Skill Learning." *The Journal of Neuroscience: The Official Journal of the Society for*

11   *Neuroscience* 16 (14): 4529–35.

12   Ladha, Cassim, K. Ladha, D. Jackson, and Patrick Olivier. 2013. "Shaker Table Validation of

13   OpenMovement AX3 Accelerometer." In *Ahmerst (ICAMPAM 2013 AMHERST): In*

14   *3rd International Conference on Ambulatory Monitoring of Physical Activity and*

15   *Movement*, 69–70.

16   Liewald, Daniel, Robert Miller, Nikos Logothetis, Hans-Joachim Wagner, and Almut Schüz.

17   2014. "Distribution of Axon Diameters in Cortical White Matter: An Electron-

18   Microscopic Study on Three Human Brains and a Macaque." *Biological Cybernetics*.

19   https://doi.org/10.1007/s00422-014-0626-2.

20   Li, Jie, Yun-Hong Ding, Josè A. Rafols, Qin Lai, James P. McAllister 2nd, and Yuchuan

21   Ding. 2005. "Increased Astrocyte Proliferation in Rats after Running Exercise."

22   *Neuroscience Letters* 386 (3): 160–64.

23   Lubans, David, Justin Richards, Charles Hillman, Guy Faulkner, Mark Beauchamp, Michael

24   Nilsson, Paul Kelly, Jordan Smith, Lauren Raine, and Stuart Biddle. 2016. "Physical

25   Activity for Cognitive and Mental Health in Youth: A Systematic Review of

Mechanisms." *Pediatrics* 138 (3). https://doi.org/10.1542/peds.2016-1642.

Luo, Yanmin, Qian Xiao, Jin Wang, Lin Jiang, Menglan Hu, Yanhong Jiang, Jing Tang, et al. 2019. "Running Exercise Protects Oligodendrocytes in the Medial Prefrontal Cortex in Chronic Unpredictable Stress Rat Model." *Translational Psychiatry* 9 (1): 322.

Lutti, Antoine, Frederic Dick, Martin I. Sereno, and Nikolaus Weiskopf. 2014. "Using High-Resolution Quantitative Mapping of R1 as an Index of Cortical Myelination." *NeuroImage* 93 Pt 2 (June): 176–88.

Miller, Karla L., Fidel Alfaro-Almagro, Neal K. Bangerter, David L. Thomas, Essa Yacoub, Junqian Xu, Andreas J. Bartsch, et al. 2016. "Multimodal Population Brain Imaging in the UK Biobank Prospective Epidemiological Study." *Nature Neuroscience*. https://doi.org/10.1038/nn.4393.

Oberheim, Nancy Ann, Takahiro Takano, Xiaoning Han, Wei He, Jane H. C. Lin, Fushun Wang, Qiwu Xu, et al. 2009. "Uniquely Hominid Features of Adult Human Astrocytes." *The Journal of Neuroscience: The Official Journal of the Society for Neuroscience* 29 (10): 3276–87.

Okell, Thomas W., Michael A. Chappell, Michael E. Kelly, and Peter Jezzard. 2013. "Cerebral Blood Flow Quantification Using Vessel-Encoded Arterial Spin Labeling." *Journal of Cerebral Blood Flow and Metabolism: Official Journal of the International Society of Cerebral Blood Flow and Metabolism* 33 (11): 1716–24.

Patenaude, Brian, Stephen M. Smith, David N. Kennedy, and Mark Jenkinson. 2011. "A Bayesian Model of Shape and Appearance for Subcortical Brain Segmentation." *NeuroImage*. https://doi.org/10.1016/j.neuroimage.2011.02.046.

Pereira, A. C., D. E. Huddleston, A. M. Brickman, A. A. Sosunov, R. Hen, G. M. McKhann, R. Sloan, F. H. Gage, T. R. Brown, and S. A. Small. 2007. "An in Vivo Correlate of Exercise-Induced Neurogenesis in the Adult Dentate Gyrus." *Proceedings of the*

National Academy of Sciences. https://doi.org/10.1073/pnas.0611721104.

Pertzov, Yoni, Mia Yuan Dong, Muy-Cheng Peich, and Masud Husain. 2012. "Forgetting What Was Where: The Fragility of Object-Location Binding." *PloS One* 7 (10): e48214.

Petersen, Anne C., Lisa Crockett, Maryse Richards, and Andrew Boxer. 1988. "A Self-Report Measure of Pubertal Status: Reliability, Validity, and Initial Norms." *Journal of Youth and Adolescence*. https://doi.org/10.1007/bf01537962.

Phillips, Lisa R. S., Gaynor Parfitt, and Alex V. Rowlands. 2013. "Calibration of the GENEA Accelerometer for Assessment of Physical Activity Intensity in Children." *Journal of Science and Medicine in Sport*. https://doi.org/10.1016/j.jsams.2012.05.013.

Piercy, Katrina L., and Richard P. Troiano. 2018. "Physical Activity Guidelines for Americans From the US Department of Health and Human Services." *Circulation. Cardiovascular Quality and Outcomes* 11 (11): e005263.

Praag, H. van, B. R. Christie, T. J. Sejnowski, and F. H. Gage. 1999. "Running Enhances Neurogenesis, Learning, and Long-Term Potentiation in Mice." *Proceedings of the National Academy of Sciences of the United States of America* 96 (23): 13427–31.

Promotion, U. S. Department of Health &. Human Services Office of Disease Prevention And Health, and US Department of Health & Human Services Office of Disease Prevention and Health Promotion. 2000. "Healthy People 2010: Understanding and Improving Health." *PsycEXTRA Dataset*. https://doi.org/10.1037/e319432004-001.

Rhyu, I. J., J. A. Bytheway, S. J. Kohler, H. Lange, K. J. Lee, J. Boklewski, K. McCormick, et al. 2010. "Effects of Aerobic Exercise Training on Cognitive Function and Cortical Vascularity in Monkeys." *Neuroscience* 167 (4): 1239–48.

Salimi-Khorshidi, Gholamreza, Gwenaëlle Douaud, Christian F. Beckmann, Matthew F. Glasser, Ludovica Griffanti, and Stephen M. Smith. 2014. "Automatic Denoising of Functional MRI Data: Combining Independent Component Analysis and Hierarchical

1   Fusion of Classifiers." *NeuroImage* 90 (April): 449–68.

2 Smith, Stephen M. 2002. "Fast Robust Automated Brain Extraction." *Human Brain Mapping*

3   17 (3): 143–55.

4 Smith, Stephen M., Thomas E. Nichols, Diego Vidaurre, Anderson M. Winkler, Timothy E.

5   J. Behrens, Matthew F. Glasser, Kamil Ugurbil, Deanna M. Barch, David C. Van Essen,

6   and Karla L. Miller. 2015. "A Positive-Negative Mode of Population Covariation Links

7   Brain Connectivity, Demographics and Behavior." *Nature Neuroscience* 18 (11): 1565–

8   67.

9 Tardif, Christine Lucas, Claudine Joëlle Gauthier, Christopher John Steele, Pierre-Louis

10   Bazin, Andreas Schäfer, Alexander Schaefer, Robert Turner, and Arno Villringer. 2016.

11   "Advanced MRI Techniques to Improve Our Understanding of Experience-Induced

12   Neuroplasticity." *NeuroImage* 131 (May): 55–72.

13 Tariq, Maira, Torben Schneider, Daniel C. Alexander, Claudia A. Gandini Wheeler-

14   Kingshott, and Hui Zhang. 2016. "Bingham-NODDI: Mapping Anisotropic Orientation

15   Dispersion of Neurites Using Diffusion MRI." *NeuroImage* 133 (June): 207–23.

16 Theil, H. 1965. "The Analysis of Disturbances in Regression Analysis." *Journal of the*

17   *American Statistical Association*. https://doi.org/10.1080/01621459.1965.10480851.

18 Thomas, Adam G., Andrea Dennis, Peter A. Bandettini, and Heidi Johansen-Berg. 2012.

19   "The Effects of Aerobic Activity on Brain Structure." *Frontiers in Psychology* 3

20   (March): 86.

21 Thomas, Adam G., Andrea Dennis, Nancy B. Rawlings, Charlotte J. Stagg, Lucy Matthews,

22   Martyn Morris, Shannon H. Kolind, et al. 2016. "Multi-Modal Characterization of Rapid

23   Anterior Hippocampal Volume Increase Associated with Aerobic Exercise."

24   *NeuroImage* 131 (May): 162–70.

25 Troiano, Richard P., James J. McClain, Robert J. Brychta, and Kong Y. Chen. 2014.

1 "Evolution of Accelerometer Methods for Physical Activity Research." *British Journal*

2 *of Sports Medicine* 48 (13): 1019–23.

3 Uda, Munehiro, Minenori Ishido, Katsuya Kami, and Mitsuhiko Masuhara. 2006. "Effects of

4 Chronic Treadmill Running on Neurogenesis in the Dentate Gyrus of the Hippocampus

5 of Adult Rat." *Brain Research* 1104 (1): 64–72.

6 Valkenborghs, Sarah Ruth, Michael Noetel, Charles H. Hillman, Michael Nilsson, Jordan J.

7 Smith, Francisco B. Ortega, and David Revalds Lubans. 2019. "The Impact of Physical

8 Activity on Brain Structure and Function in Youth: A Systematic Review." *Pediatrics*

9 144 (4). https://doi.org/10.1542/peds.2018-4032.

10 Vaynman, Shoshanna, Zhe Ying, and Fernando Gomez-Pinilla. 2004. "Hippocampal BDNF

11 Mediates the Efficacy of Exercise on Synaptic Plasticity and Cognition." *The European*

12 *Journal of Neuroscience* 20 (10): 2580–90.

13 Voss, M. W., L. Chaddock, J. S. Kim, M. VanPatter, M. B. Pontifex, L. B. Raine, N. J.

14 Cohen, C. H. Hillman, and A. F. Kramer. 2011. "Aerobic Fitness Is Associated with

15 Greater Efficiency of the Network Underlying Cognitive Control in Preadolescent

16 Children." *Neuroscience*. https://doi.org/10.1016/j.neuroscience.2011.10.009.

17 Walhovd, K. B., H. Johansen-Berg, and R. T. Káradóttir. 2014. "Unraveling the Secrets of

18 White Matter – Bridging the Gap between Cellular, Animal and Human Imaging

19 Studies." *Neuroscience*. https://doi.org/10.1016/j.neuroscience.2014.06.058.

20 Wassenaar, T. M., C. M. Wheatley, N. Beale, P. Salvan, A. Meaney, J. B. Possee, K. E.

21 Atherton, J. L. Duda, H. Dawes, and H. Johansen-Berg. 2019. "Effects of a Programme

22 of Vigorous Physical Activity during Secondary School Physical Education on

23 Academic Performance, Fitness, Cognition, Mental Health and the Brain of Adolescents

24 (Fit to Study): Study Protocol for a Cluster-Randomised Trial." *Trials* 20 (1): 189.

25 Weiskopf, Nikolaus, John Suckling, Guy Williams, Marta M. Correia, Becky Inkster, Roger

1   Tait, Cinly Ooi, Edward T. Bullmore, and Antoine Lutti. 2013. "Quantitative Multi-

2   Parameter Mapping of R1, PD*, MT, and R2* at 3T: A Multi-Center Validation."

3   *Frontiers in Neuroscience*. https://doi.org/10.3389/fnins.2013.00095.

4   Winkler, Anderson M., Olivier Renaud, Stephen M. Smith, and Thomas E. Nichols. 2020.

5   "Permutation Inference for Canonical Correlation Analysis." *arXiv [stat.ME]*. arXiv.

6   http://arxiv.org/abs/2002.10046.

7   Winkler, Anderson M., Gerard R. Ridgway, Gwenaëlle Douaud, Thomas E. Nichols, and

8   Stephen M. Smith. 2016. "Faster Permutation Inference in Brain Imaging." *NeuroImage*

9   141 (November): 502–16.

10   Winkler, Anderson M., Matthew A. Webster, Diego Vidaurre, Thomas E. Nichols, and

11   Stephen M. Smith. 2015. "Multi-Level Block Permutation." *NeuroImage* 123

12   (December): 253–68.

13   World Health Organization. 2010. "Global Recommendations on Physical Activity for

14   Health." WHO Guidelines Approved by the Guidelines Review Committee. World

15   Health Organization, Geneva.

16   World Health Organization. Regional Office for Europe. 2016. *Growing Up Unequal:*

17   *Gender and Socioeconomic Differences in Young People's Health and Well-Being :*

18   *Health Behaviour in School-Aged Children (HBSC) Study : International Report from*

19   *the 2013/2014 Survey*. World Health Organization.

20   Zatorre, Robert J., R. Douglas Fields, and Heidi Johansen-Berg. 2012. "Plasticity in Gray and

21   White: Neuroimaging Changes in Brain Structure during Learning." *Nature*

22   *Neuroscience* 15 (4): 528–36.

23   Zhang, Y., M. Brady, and S. Smith. 2001. "Segmentation of Brain MR Images through a

24   Hidden Markov Random Field Model and the Expectation-Maximization Algorithm."

25   *IEEE Transactions on Medical Imaging* 20 (1): 45–57.

26

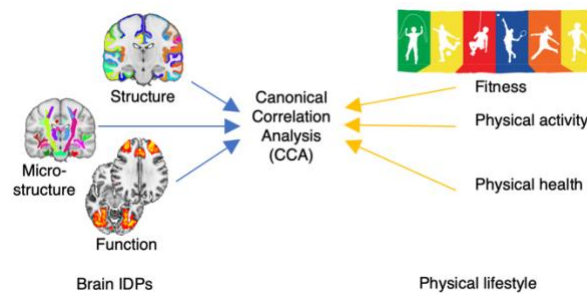1   **Figure legends**

2

3

4   **Figure 1 Summary of statistical analysis.** In order to test the individual covariation between

5   brain IDPs and physical measures of fitness, physical activity and physical health, we aimed

6   to identify one single mode of covariation using canonical correlation analysis (CCA), while

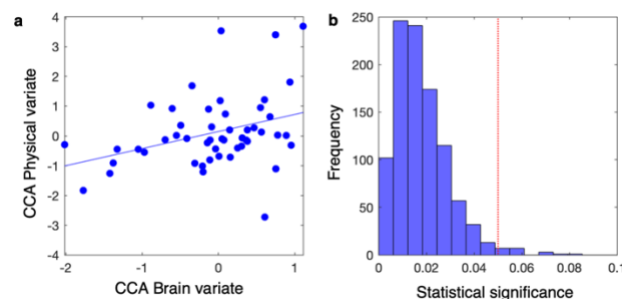7   taking into account the hierarchical structure represented by schools.

8

9

10   **Figure 2 Mode of brain – physical covariation across pupils.** The results from canonical

11   correlation analysis (CCA) highlight one significant mode of brain – physical covariation

12   across pupils. **a**) Showing scatter plot of cross-validated canonical variates between brain IDP

13   scores and physical scores, each dot represents a pupil (cross-validated CCA: rho = 0.34).

14   Statistical significance of CCA was assessed 1,000 times, each time comparing the real value

15   against 1,000 block-aware permutations taking into account school structure. **b**) Showing

16   distribution of statistical significance values. The final significance value was assessed as the

17   average of this distribution (p-value = 0.0130). Red dashed line represents cut-off of

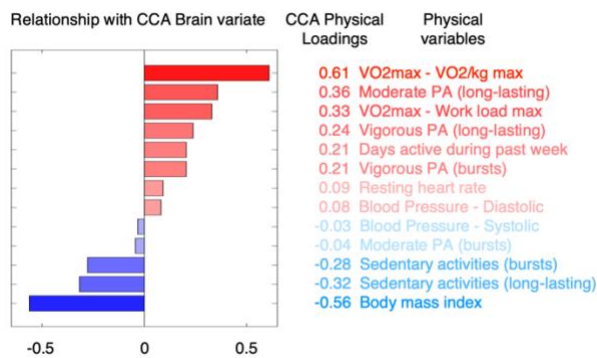18   statistical significance of alpha = 0.05.

19

1

2 **Figure 3 Physical phenotype linked to the brain – physical mode of covariation.** Bar plot

3 representing the coefficient structure of physical phenotype (formally CCA Physical

4 loadings). Each coefficient represents the relationship between each physical metric and

5 subjects' brain IDP scores (or CCA Brain variate). Bar plot and variable ranking are matched

6 and color-coded in red/blue in accordance to a positive/negative relationship with the mode

7 of covariation (the magnitude of involvement is further represented through transparency).
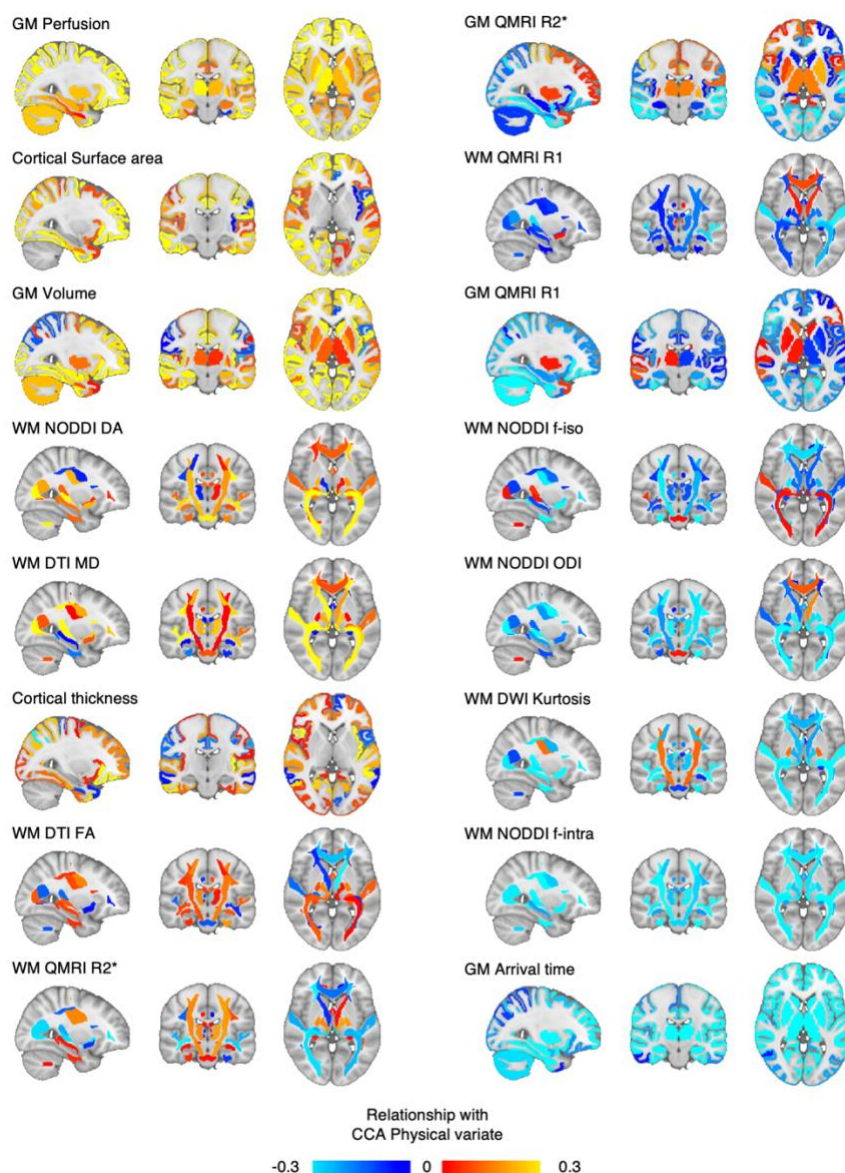
8

1

Figure 4 Structural IDPs and their relationship with the identified phenotype of physically active lifestyle. Showing for each MRI metric and for each structural ROI, thus for all structural IDPs, the relationship with the identified phenotype of active lifestyle. Hot colors represent a positive relationship with the physical phenotype; cold colors represent a negative relationship. Structural maps are ranked from top to bottom (left column to right) in accordance to *average* CCA W Brain.
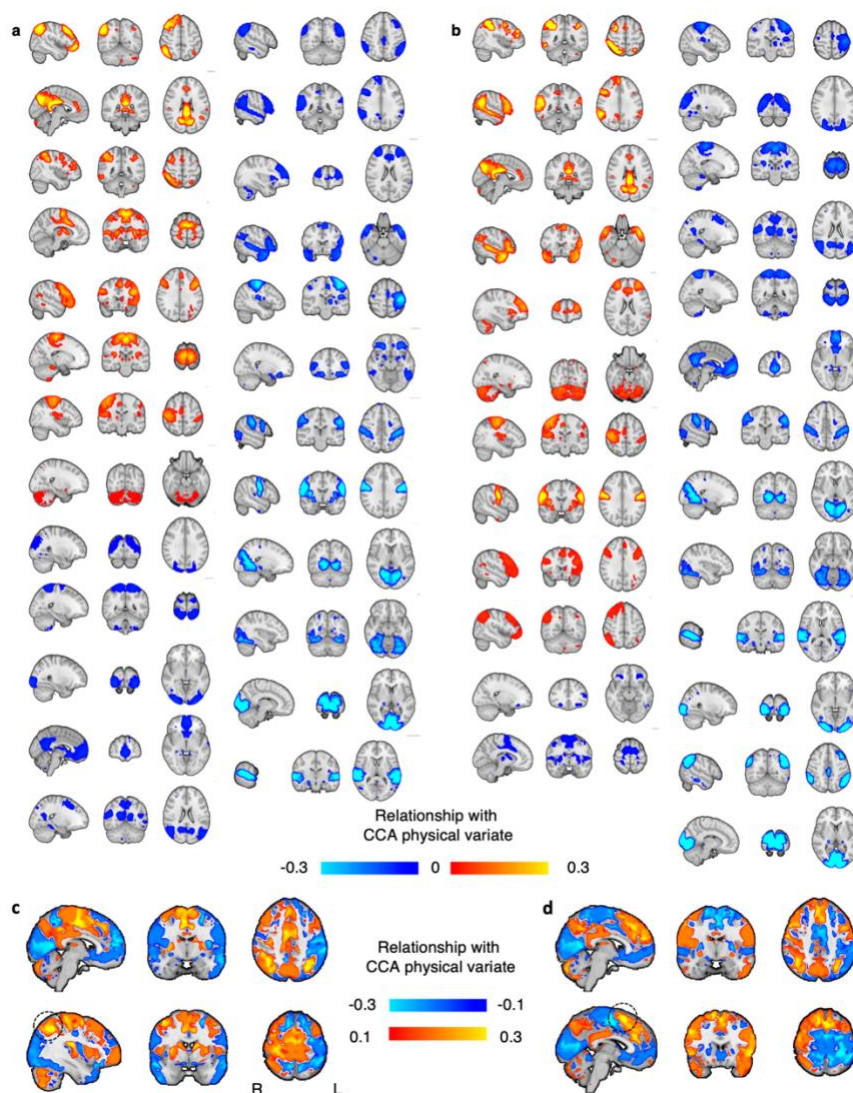
Figure 5 Functional IDPs and their relationship with the identified phenotype of physically active lifestyle. Showing for each resting state brain network (RSN), and for both metrics functional connectivity **a**) and amplitude **b**), the relationship with the identified phenotype of active lifestyle. Hot colors represent a positive relationship with the physical phenotype; cold colors represent a negative relationship. To aid interpretation, for each RSN, its CCA Brain loading was multiplied by the group RSN map. RSN are here ranked from top-to-bottom in accordance to their CCA Brain loadings. We then concatenated all RSNs maps in a 4D file and computed the mean and standard deviation across RSNs, separately for both functional connectivity and amplitude. **c**) Normalised mean of CCA Brain loadings for RSNs functional connectivity. **d**) Normalised mean of CCA Brain loadings for RSNs amplitude.

1 For **c**) and **d**), the top row shows the same brain coordinates, whilst the bottom row shows the

2 respective peak of greater CCA Brain loadings. Dashed circle in **c**) and **d**) represents the peak
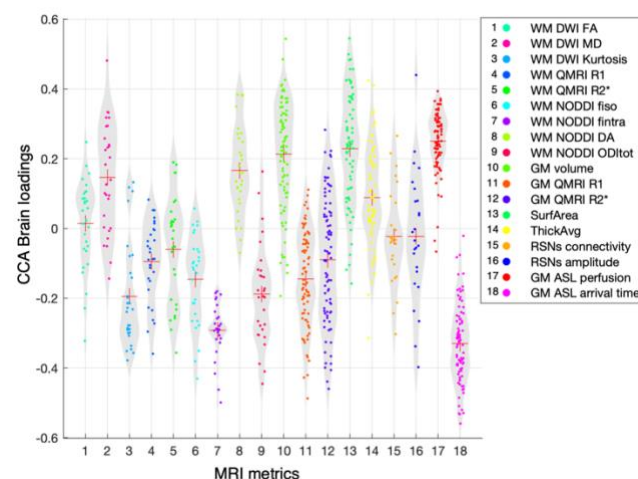
3 value.

4

5

6 **Figure 6 Relationship with physical lifestyle phenotype for all brain IDPs.** Showing the

7 CCA Brain loadings for all 859 brain IDPs divided into each MRI metric. Each dot represents

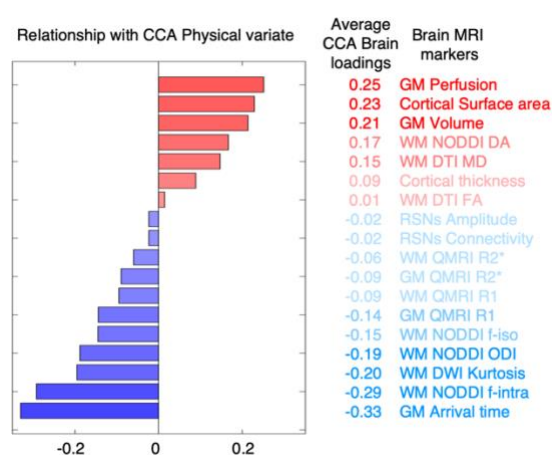8 one single IDP.

9

10

11 **Figure 7 Brain phenotype linked to the brain – physical mode of covariation.** Bar plot

12 representing the *average* CCA Brain loadings. Each coefficient represents the relationship

13 between each MRI metric (average across ROIs) and pupils' physical lifestyle scores. Bar

1   plot and variable ranking are matched and color-coded in red/blue in accordance to a

2   positive/negative relationship with the mode of covariation (the magnitude of involvement is

3   further represented through transparency).

4

5   **Table legends**

6

7   **Table 1 Demographics and socioeconomic status.**

	Mean	Standard deviation
Demographics		
Age (years)	12	0.27
Sex (female)	26 (52%)	/
Pubertal development level	2.22	0.59
Index of Multiple Deprivation (Decile)	7.82	1.96

8

9   **Table 2 Sampling frequency by school.**

School	Number of pupils	%
A	1	2
B	2	4
C	10	20
D	6	12
E	8	16
F	1	2
G	1	2
H	1	2
I	13	26
L	7	14

10

11   **Table 3 Descriptives of cognitive skills, reported mental health, and reported general**

12   **health.**

43

	Mean	Standard deviation
Cognition		
Associative task (correct valid answers (%))	71	11
Task switching (switch cost (ms))	548	333
Object location task (Identification errors 8s-delay)	11	4
Mental health (SDQ questionnaire)		
Prosocial Scale	8	1.4
Hyperactivity Scale	4	2.5
Conduct Scale	2	1.5
Peer Scale	2	1.9
Emotional Scale	3	2.3
General Health (HSBC questionnaire)		
Life satisfaction	8	1.6
Self-Rated Health	4	0.9
Multiple health complaints	13	4.8

1

2 **Table 4 List of MRI modalities and MRI metrics used to define IDPs of brain function**

3 **and structure.** 5 MRI sequences were used to quantify 18 different MRI metrics. Specific

4 sets of ROIs were then used for each MRI metric in order to extract whole-brain MM IDPs

5 quantifying brain structure, microstructure, function, myelin content, and blood perfusion.

Brain tissue	MRI modality	Parameter
Grey matter (cortex & sub-cortex)	Structural	Volume (VBM-like)
	Quantitative	R1
	Quantitative	R2*
	Arterial Spin Labelling	Perfusion
	Arterial Spin Labelling	Arrival time
Cortex	Structural	Surface area
	Structural	Surface thickness
BOLD activity	rs-fMRI	Functional connectivity
	rs-fMRI	Amplitude

	Diffusion	DTI - FA
	Diffusion	DTI - MD
	Diffusion	DTI - Kurtosis
	Quantitative	R1
White matter	Quantitative	R2*
	Diffusion	NODDI f-iso
	Diffusion	NODDI f-intra
	Diffusion	NODDI DA
	Diffusion	NODDI ODI

1

2   **Table 5 Descriptives of physical variables.** 13 measures of physical activity, fitness, and

3   physical health were considered in testing the relationship with brain IDPs. Here we report

4   mean and standard deviation (prior of correcting for demographics and socioeconomic

5   status).

6

	Mean	Standard deviation
VO2max - VO2/kg max (ml/min/kg)	37.2	8.5
VO2max - Work load max (Watts)	137.8	25.9
Vigorous PA (bursts) (min per week)	41.0	34.2
Moderate PA (bursts) (min per week)	247.0	106.0
Sedentary activities (bursts) (min per week)	4075.0	993.0
Vigorous PA (long-lasting) (min per week)	10.0	14.0
Moderate PA (long-lasting) (min per week)	320.0	167.0
Sedentary activities (long-lasting) (min per week)	3502.0	369.0
Days active during past week	4.9	1.8
Body mass index	19.5	4.1
Resting heart rate (bpm)	75.0	12.0
Blood Pressure - Systolic (mm Hg)	106.0	10.0
Blood Pressure - Diastolic (mm Hg)	73.0	7.0

7